J|A|C|S
ARTICLES
Published on Web 02/07/2004

High-Efficiency Poly(*p*-phenylenevinylene)-Based Copolymers Containing an Oxadiazole Pendant Group for Light-Emitting Diodes

Sung-Ho Jin,*,† Mock-Yeon Kim,† Jin Young Kim,‡ Kwanghee Lee,‡ and Yeong-Soon Gal§

Contribution from the Departments of Chemistry Education and Physics, and Center for Plastic Information System, Pusan National University, Busan 609-735, Korea, and Polymer Chemistry Laboratory, Kyungil University, Hayang 712-701, Korea

Received June 28, 2003; E-mail: shjin@pusan.ac.kr

Abstract: A new series of high brightness and luminance efficient poly(*p*-phenylenevinylene) (PPV)-based electroluminescent (EL) polymers, poly[2-{4-[5-(4-(3,7-dimethyloctyloxy)phenyl)-1,3,4-oxadiazole-2-yl]phenyloxy}-1,4-phenylenevinylene] (Oxa-PPV), poly[2-{2-((3,7-dimethyloctyl)oxy)phenoxy}-1,4-phenylenevinylene] (DMOP-PPV), and their corresponding random copolymers, poly{[2-{4-[5-(4-(3,7-dimethyloctyloxy)-phenyl)-1,3,4-oxadiazole-2-yl]phenyloxy}-1,4-phenylenevinylene]-*co*-[2-{2-((3,7-dimethyloctyl)oxy) phenoxy}-1,4-phenylenevinylene]} (Oxa-PPV-*co*-DMOP-PPV), with an electron-deficient 1,3,4-oxadiazole unit on the side groups, were synthesized through the Gilch polymerization method. The newly designed and synthesized asymmetric molecular structures of Oxa-PPV, DMOP-PPV, and Oxa-PPV-*co*-DMOP-PPV were completely soluble in common organic solvents, and defect-free optical thin film was easily spin-coated onto the indium tin oxide (ITO) substrate. Oxa-PPV shows a high glass transition temperature (T_g), which might be an advantage for long time operation of polymer light-emitting diodes (PLEDs). Double-layer LEDs with an ITO/PEDOT/polymer/Al configuration were fabricated by using those polymers. Electrooptical properties and device performance could be adjusted by introducing the Oxa-PPV content in the copolymers. The emission colors could be tuned from green to yellowish-orange via intramolecular energy transfer. The improved device performance of Oxa-PPV over DMOP-PPV and Oxa-PPV-*co*-DMOP-PPV may be due to better electron injection and charge balance between holes and electrons and also efficient intramolecular energy transfer from 1,3,4-oxadiazole units to PPV backbones. The maximum brightness and the luminance efficiency of Oxa-PPV were up to 19395 cd/m^2 at 14 V and 21.1 cd/A at 5930 cd/m^2. The maximum luminance efficiency of Oxa-PPV is ranked the highest value among the PPV derivatives to date.

Introduction

Since the report of polymer light-emitting diodes (PLEDs) based on poly(*p*-phenylenevinylene) (PPV) by the Cambridge group, π-conjugated polymers have attracted much attention because of their good ability to form thin films, good mechanical properties, excellent luminescence, etc.[1,2] Yet a problem of π-conjugated polymers is that electron injection is much more difficult than hole injection, resulting in the imbalance of rates for electron and hole injection from negative and positive contacts and a shift of the recombination zone toward the region near the interface of the polymer/cathode.[3] The luminance efficiency of the device determined by the amount of charge carrier injection, the probability of the capture of charges, and the ratio of singlet excitons formed is limited.[4−6] A balance of the rates of injection of electrons and holes from opposite contacts into the device is crucial in achieving high electroluminescent efficiency.[7,8] The use of a metal with a low work function such as calcium, magnesium, or lithium as cathode can lower the charge injection barrier at the cathode to improve the luminance efficiency by balancing injected electrons and holes.[9−11] However, these metals have high chemical reactivity

† Department of Chemistry Education and Center for Plastic Information System, Pusan National University.
‡ Department of Physics and Center for Plastic Information System, Pusan National University.
§ Kyungil University.

(1) Burroughes, J. H.; Bradley, D. D. C.; Brown, A. R.; Marks, R. N.; Mackay, K.; Friend, R. H.; Burns P. L.; Holmes, A. B. *Nature* **1990**, *347*, 539−541.
(2) Bernius, M. T.; Inbasekaran, M.; O'Brien, J.; Wu, W. *Adv. Mater*. **2000**, *12*, 1737−1750.
(3) Meng, H.; Yu, W. L.; Huang, W. *Macromolecules* **1999**, *32*, 8841−8847.
(4) Peng, Z.; Zhang, J. *Chem. Mater*. **1999**, *11*, 1138−1143.
(5) Lee, D. W.; Kwon, K. Y.; Jin, J. I.; Park, Y. S.; Kim, Y. R.; Hwang, I. W. *Chem. Mater*. **2001**, *13*, 565−574.
(6) Lee, Y. Z.; Chen, X.; Chen, S. A.; Wei, P. K.; Fann, W. S. *J. Am. Chem. Soc.* **2001**, *123*, 2296−2307.
(7) Greenham, S. C.; Moratti; S. C.; Bradley, D. D. C.; Friend, R. H.; Holmes, A. B. *Nature* **1993**, *365*, 628−630.
(8) Garten, F.; Hilberer, A.; Cacialli, F.; Essenlink, E.; van Dam, Y.; Schlatmann, B.; Friend, R. H.; Klapwijk, T. M.; Hadziioannou, G. *Adv. Mater*. **1997**, *9*, 127−131.
(9) Braun, D.; Heeger, A. J. *Thin Solid Films* **1992**, *216*, 96−98.
(10) Parker, I. D. *J. Appl. Phys.* **1994**, *75*, 1656−1666.
(11) Bao, Z.; Peng, Z.; Galvin, M. E.; Chandross, E. A. *Chem. Mater*. **1998**, *10*, 1201−1204.

10.1021/ja036955+ CCC: $27.50

to oxygen and moisture, which limits their practicality. Multilayer devices have an electron transport layer (ETL) between a light-emitting layer and a negative electrode and have been found to be more efficient than single-layer devices.[12] However, multilayer devices require careful selection of solvent so that the solution of an electron transport material will not damage the previous light-emitting layer. Besides, the method could cause space charges and tunneling of accumulated holes[13,14] and increase the turn-on voltage. Another strategy to improve the device efficiency is use of a blend of electron transport material with EL polymer. The unavoidable drawback to this approach is that phase separation[15,16] between the two different kinds of materials might happen, which could accelerate a rate of recrystallization or aggregate formation by generated heat during the device operation. Therefore, the lifetime and stability of the devices are reduced. To solve the problems of previous methods for improving the luminance efficiency, many research groups have introduced electron transport moieties on the side chain of polymer backbones or polymer main chains.[17−22] One of the most widely used electron transport moieties is aromatic 1,3,4-oxadiazole-based compounds with high electron affinities, which facilitate electron transport and injection. For such a purpose, we designed and synthesized novel PPV derivatives containing 1,3,4-oxadiazole pendant groups. In our previous work, we have synthesized PPV derivatives with alkylsilylphenyl and alkyloxyphenoxy groups as side chains and poly(9,9-di-*n*-octylfluorenyl-2,7-vinylene) (PFV) derivatives, which showed the high performance of PLED.[23−27] In this paper, we report the synthesis and characterization of PPV derivatives with a 1,3,4-oxadiazole moiety as a side chain. The 1,3,4-oxadiazole units are incorporated between the phenoxy and alkoxyphenyl substituents to improve the solubility and EL characteristics. The resulting EL polymers were synthesized by the Gilch polymerization method for high molecular weight, easy purification, narrow polydispersity, and good thermal stability.

Experimental Section

Synthesis of Ethyl 4-(2,5-Dimethylphenoxy)benzoate, 1. In a 250 mL three-neck flask, 2,5-dimethylphenol (16.7 g, 137 mmol) and ethyl 4-fluorobenzoate (23 g, 137 mmol) were dissolved in 100 mL of DMF, and then potassium *tert*-butoxide (18.4 g, 164 mmol) was added at room temperature with stirring. The mixture was heated to 150 °C and kept at reflux for 10 h. The reaction mixture was cooled to room temperature, poured into excess water, and extracted with ether. The combined organic layers were washed several times further with water, dried over anhydrous $MgSO_4$, and filtered. The solvent was removed by evaporation under reduced pressure. The product was purified by column chromatography on silica gel using hexane/dichloromethane (1:1) as an eluent to give ethyl 4-(2,5-dimethylphenoxy)benzoate, **1** (25 g, 68%). ^{1}H NMR ($CDCl_3$, δ ppm): 1.34−1.41 (t, 3H, CH_3), 2.12, 2.30 (s, 6H, $2CH_3$ on aromatic ring), 4.29−4.40 (q, 2H, $-OCH_2-$), 6.79, 6.84−6.89, 6.92−6.96, 7.13−7.17, 7.96−8.00 (m, 7H, aromatic protons).

Synthesis of 4-(2,5-Dimethylphenoxy)benzohydrazide, 2. In a 250 mL three-neck flask, hydrazine monohydrate (26 g, 518 mmol) was dissolved in 30 mL of ethanol. Ethyl 4-(2,5-dimethylphenoxy)benzoate, **1** (20 g, 74 mmol), was added dropwise and stirred at 90 °C for 17 h. After confirmation of the disappearance of ethyl 4-(2,5-dimethylphenoxy)benzoate, **1**, by TLC, the mixture was cooled to room temperature and then recrystallized from methanol. A crystal product was washed several times further with hexane. A white crystal product, 4-(2,5-dimethylphenoxy)benzohydrazide, **2**, was obtained (14 g, 75%). ^{1}H NMR ($CDCl_3$, δ ppm): 2.12, 2.30 (s, 6H, $2CH_3$ on aromatic ring), 4.0−4.2 (b, 2H, NH_2), 7.20−7.40 (b, 1H, NH), 6.78, 6.84−6.96, 7.13−7.17, 7.65−7.72 (m, 7H, aromatic protons).

Synthesis of *N*-{4-[(3,7-Dimethyloctyl)oxy]benzoyl}-4-(2,3-dimethylphenoxy)benzohydrazide, 3. In a 250 mL three-neck flask, 4-(2,5-dimethylphenoxy)benzohydrazide, **2** (4.4 g, 17 mmol), and triethylamine (1.7 g, 17 mmol) were dissolved in 50 mL of dichloromethane, and 4-(3,7-dimethyloctyloxy)benzoyl chloride (5.1 g, 17 mmol) was added dropwise. The mixture was stirred at room temperature for 4 h and then extracted with water and dichloromethane several times. The organic layers were dried over anhydrous $MgSO_4$ and filtered. The solvent was removed by evaporation under reduced pressure. The product was recrystallized from methanol and washed several times with hexane to give white crystals of *N*-{4-[(3,7-dimethyloctyl)oxy]benzoyl}-4-(2,3-dimethylphenoxy)benzohydrazide, **3** (8.5 g, 97%). ^{1}H NMR ($CDCl_3$, δ ppm): 0.84−0.88 (d, 6H, $2CH_3$), 0.92−0.95 (d, 3H, CH_3), 1.16−1.85 (m, 10H, $4CH_2$, 2CH), 2.11, 2.30 (s, 6H, $2CH_3$ on aromatic ring), 3.98−4.05 (t, 2H, OCH_2), 6.78−6.96, 7.12−7.16, 7.78−7.83 (m, 11H, aromatic protons), 9.35−9.48 (d, d, 2H, NH).

Synthesis of 2-{4-[(3,7-Dimethyloctyl)oxy]phenyl}-5-(4-(2,5-dimethylphenoxy)phenyl-1,3,4-oxadiazole, 4. To a 250 mL three-neck flask were added *N*-{4-[(3,7-dimethyloctyl)oxy]benzoyl}-4-(2,3-dimethylphenoxy)benzohydrazide, **3** (4 g, 7.7 mmol), 50 mL of benzene, and $SOCl_2$ (3.7 g, 31 mmol), and the mixture was refluxed at 120 °C for 4 h and then cooled to room temperature. The solvent and $SOCl_2$ were removed by evaporation under reduced pressure, and then the reaction mixture was poured into excess water and extracted with chloroform. The combined organic layers were washed several times further with water, dried over anhydrous $MgSO_4$, and filtered. The solvent was removed by evaporation under reduced pressure. The crude product was purified by column chromatography on silica gel using hexane as an eluent to give **4** (3.7 g, 95%). ^{1}H NMR ($CDCl_3$, δ ppm): 0.85−0.89 (d, 6H, $2CH_3$), 0.94−0.97 (d, 3H, CH_3), 1.18−1.88 (m, 10H, $4CH_2$, 2CH), 2.15, 2.31 (s, 6H, $2CH_3$ on aromatic ring), 4.03−4.10 (t, 2H, OCH_2), 6.82, 6.93−7.03, 7.14−7.19, 8.01−8.08 (m, 11H, aromatic protons).

Synthesis of 2-{4-[2,5-Bis(bromomethyl)phenoxy]phenyl-5-{4-[(3,7-dimethyloctyl)oxy]phenyl}-1,3,4-oxadiazole, 5. To a 250 mL three-neck flask were added 2-{4-[(3,7-dimethyloctyl)oxy]phenyl}-5-(4-(2,5-dimethylphenoxy)phenyl-1,3,4-oxadiazole, **4** (5.8 g, 11.6 mmol), *N*-bromosuccinimide (NBS) (4.6 g, 25.6 mmol), catalytic amounts of benzoyl peroxide (BPO), and 100 mL of benzene. The mixture was refluxed and stirred until succinimide was on top of the solution. After

(12) Rothberg, L. R.; Lovinger, A. J. *J. Mater. Res.* **1996**, *11*, 3174−3187.
(13) Brutting, W.; Berleb, S.; Egerer, G.; Schwoerer, M.; Wehrmann, R.; Elschner, A. *Synth. Met.* **1997**, *91*, 325−327.
(14) Heischkel, Y.; Schmidt, H. W. *Macromol. Chem. Phys.* **1998**, *199*, 869−880.
(15) Strukelj, M.; Miller, T. M.; Papadimitrakopoulos, F.; Sehwan, S. *J. Am. Chem. Soc.* **1995**, *117*, 11976−11983.
(16) Halls, J. J. M.; Walsh, C. A.; Greenham, N. C.; Marseglia, E. a.; Friend, R. H.; Moratti, S. C.; Holmes, A. B. *Nature* **1995**, *376*, 498−500.
(17) Li, X. C.; Cacialli, F.; Giles, M.; Gruner, J.; Friend, R. H.; Holmes, A. B.; Moratti, S. C.; Yong, T. M. *Adv. Mater.* **1995**, *7*, 898−900.
(18) Song, S. Y.; Jang, M. S.; Shim, H. K.; Hwang, D. H.; Zyung, T. *Macromolecules* **1999**, *32*, 1482−1487.
(19) Hedrick, J. L.; Tweig, T. *Macromolecules* **1992**, *25*, 2021−2025.
(20) Chung, S. J.; Kwon, K. U.; Lee, S. W.; Jin, J. I.; Lee, C. H.; Lee, C. E.; Park, Y. *Adv. Mater.* **1998**, *10*, 1112−1116.
(21) Boyd, T. J.; Geerts, Y.; Lee, J. K.; Fogg, D. E.; Lavoie, G. G.; Schrock, R. R.; Rubner, M. F. *Macromolecules* **1997**, *30*, 3553−3559.
(22) Strukelj, M.; Papadimitrakopoulos, F.; Miller, T. M.; Rothberg, L. J. *Science* **1995**, *267*, 1969−1972.
(23) Lee, J. H.; Yu, H. S.; Kim, W.; Gal, Y. S.; Park, J. H.; Jin, S. H. *J. Polym. Sci., Part A: Polym. Chem.* **2000**, *38*, 4185−4193.
(24) Jin, S. H.; Jang, M. S.; Suh, H. S.; Cho, H. N.; Lee, J. H.; Gal, Y. S. *Chem. Mater.* **2002**, *14*, 643−650.
(25) Jin, S. H.; Kang, S. Y.; Yeom, I. S.; Kim, J. Y.; Park, S. H.; Lee, K. H.; Gal, Y. S.; Cho, H. N. *Chem. Mater.* **2002**, *14*, 5090−5097.
(26) Jin, S. H.; Park, H. J.; Kim, J. Y.; Lee, K.; Lee, S. P.; Moon, D. K.; Lee, H. J.; Gal,Y. S. *Macromolecules* **2002**, *35*, 7532−7534.
(27) Jin, S. H.; Kang, S. Y.; Kim, M. Y.; Yoon, U. C.; Kim, J. Y.; Lee, K. H.; Gal, Y. S. *Macromolecules* **2003**, *36*, 3841−3847.

Scheme 1. Synthetic Routes for the Monomer and Polymers

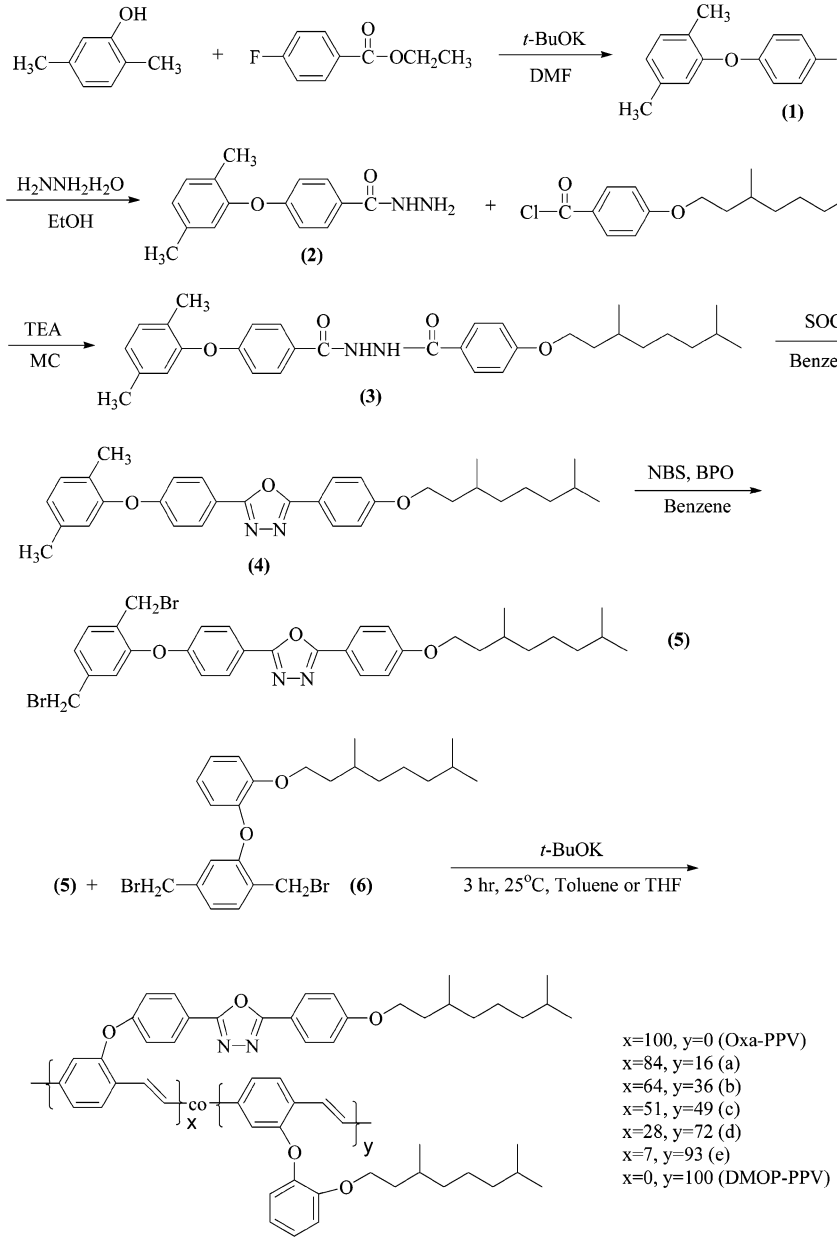

confirmation of the disappearance of the 2-{4-[(3,7-dimethyloctyl)oxy]-phenyl}-5-(4-(2,5-dimethylphenoxy)phenyl-1,3,4-oxadiazole, **4**, by TLC, the mixture was cooled to room temperature. The succinimide was filtered off, and the mother liquor was poured into excess water and extracted with dichloromethane. The combined organic layers were washed several times further with water, dried over anhydrous $MgSO_4$, and filtered. The solvent was removed by evaporation under reduced pressure. The product was purified by column chromatography on silica gel using hexane to give 2-{4-[2,5-bis(bromomethyl)phenoxy]phenyl-5{4-[(3,7-dimethyloctyl)oxy]phenyl}-1,3,4-oxadiazole, **5** (3.2 g, 41%). ^{1}H NMR ($CDCl_3$, δ ppm): 0.84−0.88 (d, 6H, $2CH_3$), 0.93−0.96 (d, 3H, CH_3), 1.17−1.88 (m, 10H, $4CH_2$, 2CH), 4.06−4.12 (t, 2H, OCH_2), 4.40, 4.54 (s, 4H, $2CH_2Br$ on aromatic ring), 6.97−7.03, 7.11−7.21, 7.43−7.48, 8.01−8.14 (m, 11H, aromatic protons). ^{13}C NMR ($CDCl_3$, δ ppm): 19.7, 22.6, 27.0, 28.0, 29.9, 32.0, 36.0, 37.3, 39.2, 66.7, 115.0, 116.1, 118.8, 119.5, 120.1, 125.3, 128.7, 129.7, 132.0, 140.4, 154.2, 159.6, 162.0. Anal. Calcd for $C_{32}H_{36}Br_2N_2O_3$: C, 58.55; H, 5.53; N, 4.27. Found: C, 58.14; H, 5.86; N, 4.01.

Synthesis of Poly[2-{4-[5-(4-(3,7-dimethyloctyloxy)phenyl)-1,3,4-oxadiazole-2-yl]phenyloxy}-1,4-phenylenevinylene] (Oxa-PPV). To a 100 mL Schlenk flask dried with a stream of hot air and flushed with N_2 was added monomer, **5** (0.3 g, 0.5 mmol), and then it was dried and flushed with N_2 again and dissolved in 30 mL of dry toluene. A solution of potassium *tert*-butoxide in THF (2.7 mL, 1.0 M) was then added at a rate of 5.5 mL/h via syringe pump. After complete addition of base, the reaction was stirred at room temperature for 4 h. To terminate the polymerization reaction, monobrominated byproduct, 2-{4-[5-(bromomethyl)-2-methylphenoxy]phenyl}-5-{4-[(3,7-dimethyl-octyl)oxy]phenyl}-1,3,4-oxadiazole, was added to the reaction mixture and further stirred for 1 h. The reaction mixture changed color from colorless to yellow to orange, and the viscosity increased. The reaction mixture was poured into 300 mL of methanol to precipitate the polymer. The collected polymer was further purified by Soxhlet extraction through methanol to remove the low molecular weight oligomers and inorganic impurities. The resulting polymer was redissolved in chloroform and washed several times further with water. The solvent moieties were evaporated with a rotary evaporator and again reprecipitated into 300 mL of methanol. The precipitated polymer was collected by suction filtration and dried in a vacuum oven to yield 0.16 mg (70%) of Oxa-PPV. ^{1}H NMR ($CDCl_3$, δ ppm): 0.72−1.00 (br,

9H, $3CH_3$), 1.02−1.40 (br, 6H, $(CH_2)_3$), 1.57 (br, 4H, 2CH, $-CH_2-$), 3.90−4.12 (br, 2H, $-OCH_2$), 6.55−7.40, 7.80−8.15 (br, 13H, aromatic protons and vinylic protons). Anal. Calcd for $C_{32}H_{34}N_2O_3$: C, 77.70; H, 6.93; N, 5.66. Found: C, 75.66; H, 7.25; N, 5.31.

Poly[2-{2-((3,7-dimethyloctyl)oxy)phenoxy}-1,4-phenylenevinylene], DMOP-PPV, and their corresponding random copolymers, poly-{[2-{4-[5-(4-(3,7-dimethyloctyloxy)phenyl)-1,3,4-oxadiazole-2-yl]phenyloxy}-1,4-phenylenevinylene]-*co*-[2-{2-((3,7-dimethyloctyl) oxy)-phenoxy}-1,4-phenylenevinylene]}, Oxa-PPV-*co*-DMOP-PPV, with various feed ratios of DMOP-PPV content were synthesized and purified by a method similar to that used for Oxa-PPV.

Results and Discussion

Synthesis and Characterization. Molecules and polymers with 1,3,4-oxadiazole derivatives are the classes of electron injection and hole blocking materials. The synthetic routes for the 1,3,4-oxadiazole containing monomer, corresponding homopolymer, and their copolymers with various compositions of DMOP-PPV are depicted in Scheme 1. Monomer with a 1,3,4-oxadiazole side chain was synthesized in five steps. Ethyl 4-(2,5-dimethylphenoxy)benzoate, **1**, was synthesized by the reaction of ethyl 4-fluorobenzoate with 2,5-dimethylphenol in the presence of potassium *tert*-butoxide in DMF solvent. The ester compound, **1**, was treated with hydrazine monohydrate to give the hydrazide, **2**, compound. Condensation of hydrazide, **2**, with 2,7-dimethyloctyloxybenzoyl chloride yielded the bis-(dihydrazide) derivative, **3**, in almost quantitative yield. Ring closure of the bis(dihydrazide) derivative with thionyl chloride in benzene solvent led to the 1,3,4-oxadiazole unit as a pendant group, **4**. The newly designed monomer was obtained via bromination of compound **4** in the presence of AIBN and was purified by column chromatography. The synthesis of 1,4-bis-(bromomethyl)-2-{2-[(3,7-dimethyloctyl)oxy] phenoxy}benzene, **6**, was described elsewhere.[25] The synthetic strategy of the present monomer, **5**, is introduction of the 1,3,4-oxadiazole unit as an ether linkage to improve the solubility of the corresponding EL polymers. The comonomer, **6**, was also linked to the 3,7-dimethyloctyloxyphenyl group in the bis(bromomethyl)benzene backbone via an oxygen atom, which induced the molecular similarity between the two monomers. Homopolymerization of monomer **5** was performed with an excess of potassium *tert*-butoxide in dry toluene under nitrogen atmosphere. To improve the device performance of PLEDs and tune the electrooptical properties of Oxa-PPV, we copolymerized the 2-{4-[2,5-bis-(bromomethyl)phenoxy]phenyl-5{4-[(3,7-dimethyloctyl)oxy]-phenyl}-1,3,4-oxadiazole, **5**, with various feed ratios of 1,4-bis(bromomethyl)-2-{2-[(3,7-dimethyloctyl)oxy]phenoxy}-benzene, **6**, in THF. During the polymerization, the viscosity of the reaction mixture was increased without any precipitation, and intense fluorescent light was observed. A small amount of monobrominated byproduct, 2-{4-[5-(bromomethyl)-2-methylphenoxy]phenyl}-5-{4-[(3,7-dimethyloctyl)oxy]phenyl}-1,3,4-oxadiazole, during the synthesis of monomer **5**, was added to the polymerization mixture to end-cap the polymer chain. Most of the light-emitting homopolymers with electron-withdrawing 1,3,4-oxadiazole units in side or main chains exhibit poor solubility that limits their application.[28,29] The resulting EL polymers were completely soluble in common organic solvents, such as chloroform, THF, chlorobenzene, and 1,2-dichlorobenzene. The good solubility behavior of the present EL polymers, Oxa-PPV and Oxa-PPV-*co*-DMOP-PPV, is due to the easily free rotation between the PPV backbone and side chain 1,3,4-oxadiazole units, which were linked via the oxygen atom and bent type 3,7-dimethyloctyloxy substituent to the phenoxy side group on DMOP-PPV. Most of the conjugated polymers tend to be p-type semiconductors with a much greater tendency for injecting and transporting holes than electrons. A balanced injection and transport of holes and electrons is crucial in achieving high quantum efficiency.

Table 1. Polymerization Results and Thermal Properties of Oxa-PPV, DMOP-PPV, and Oxa-PPV-*co*-DMOP-PPV

polymer	feed ratio (5:6)	M_w[a] ($\times 10^4$)	PDI[a]	yield (%)	DSC (T_g)	TGA[b]
Oxa-PPV	100:0	9.7	1.4	70	171	290
Oxa-PPV-*co*-DMOP-PPV (84:16)[c]	90:10	69	4.9	68	169	290
Oxa-PPV-*co*-DMOP-PPV (64:36)	70:30	38	6.5	66	126	300
Oxa-PPV-*co*-DMOP-PPV (51:49)	50:50	35	7.8	72	132	280
Oxa-PPV-*co*-DMOP-PPV (28:72)	30:70	59	8.6	79	158	370
Oxa-PPV-*co*-DMOP-PPV (7:93)	10:90	39	5.9	76	102	380
DMOP-PPV	0:100	18	4.8	70	252	320

[a] M_w and PDI values of the polymers were determined by GPC using polystyrene standards. [b] TGA was measured at a temperature of 5% weight loss for the polymers. [c] Composition ratio was determined from the ratios of phenyl protons on 1,3,4-oxadiazole and methylene next to the oxygen atom.

Table 1 summarizes the polymerization results, molecular weights, and thermal data of the Oxa-PPV, DMOP-PPV, and their copolymers, Oxa-PPV-*co*-DMOP-PPV. The weight average molecular weight (M_w) and polydispersity of the present polymers were found to be in the range of $(9.7-69) \times 10^4$ and 1.4−8.6, respectively. The structure and thermal properties of the polymers were identified by ^1H,^{13}C NMR spectroscopy, TGA, and DSC thermograms. Bromobenzylic proton peaks of monomer **5** showed two peaks at 4.40 and 4.54 ppm. These two splitting peaks are due to the asymmetric molecular structure by introduction of one electron-withdrawing 1,3,4-oxadiazole substituent into the 1,4-bis(bromomethyl)benzene unit, which gave different acidities of benzylic protons. These peaks disappeared during the polymerization, and new vinylic proton peaks appeared at 6.5−7.3 ppm together with phenyl proton peaks. Four phenyl proton and methylene proton peaks next to the 1,3,4-oxadiazole ring and oxygen atom appeared at 8 and 4.1 ppm, respectively. The compositions of copolymers were calculated from the comparison of these two peaks. The TGA thermograms, which were measured at a temperature of 5% weight loss for Oxa-PPV, DMOP-PPV, and Oxa-PPV-*co*-DMOP-PPV, revealed a thermal stability from 290 to 380 °C. It is difficult to detect the T_g value for most of the dialkyloxy-substituted PPV derivatives such as MEH-PPV and BEH-PPV. However, a distinct T_g value for Oxa-PPV, DMOP-PPV, and Oxa-PPV-*co*-DMOP-PPV was observed from 102 to 252 °C, and no melting transition was observed, which indicate that the polymers have amorphous structures. The high T_g values of present EL polymers prevent the deformation of polymer morphology and degradation of the polymer emitting layer by applied electric fields of LEDs.

(28) Huang, W.; Meng, H.; Yu, W. L.; Ga, J.; Heeger, A. J. *Adv. Mater*. **1998**, *10*, 593−596.
(29) Chen, Z. K.; Meng, H.; Lai, Y. H.; Huang, W. *Macromolecules* **1999**, *32*, 4351−4358.

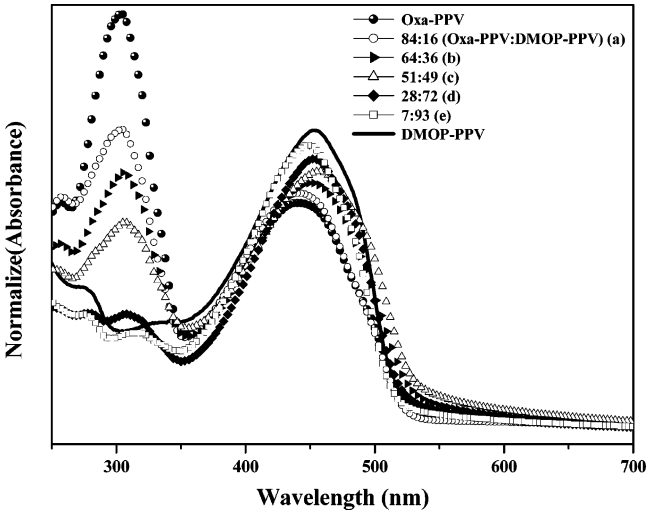

Figure 1. UV−visible absorption spectra of Oxa-PPV, DMOP-PPV, and DMOP-PPV-*co*-Oxa-PPV in the solid state.

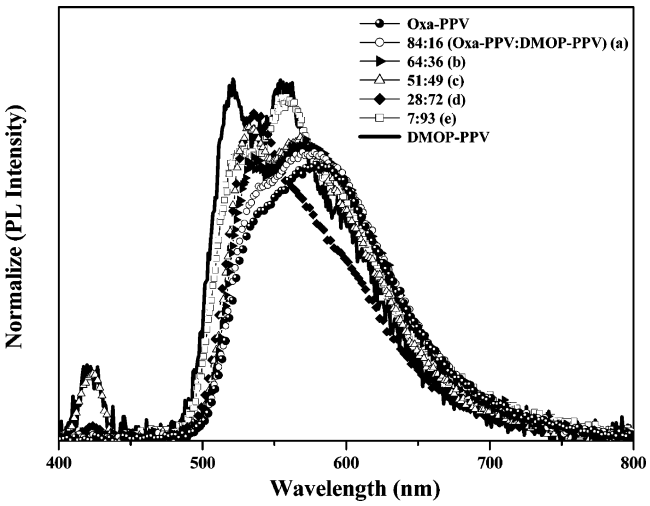

Figure 2. Photoluminescence spectra of Oxa-PPV, DMOP-PPV, and DMOP-PPV-*co*-Oxa-PPV in the solid state.

UV−Visible Absorption, Photoluminescence Spectroscopy, and Electrochemical Properties. Figure 1 shows the optical absorption spectra of Oxa-PPV, DMOP-PPV, and Oxa-PPV-*co*-DMOP-PPV with various compositions of DMOP-PPV in the solid state. The absorption spectrum of Oxa-PPV exhibited two peaks at 441 and 303 nm, which were contributed from π-conjugated main chains and 1,3,4-oxadiazole units, respectively. As the DMOP-PPV content is increased, the absorption maximum peak of the 1,3,4-oxadiazole units is decreased and the absorption λ_{max} of the $\pi-\pi^*$ transition of conjugated main chains is statistically increased. The band gap of Oxa-PPV, DMOP-PPV, and Oxa-PPV-*co*-DMOP-PPV, taken from the absorption edge spectrum, is quite different according to the compositions of copolymers. Due to the electron-withdrawing 1,3,4-oxadiazole unit, the LUMO binding energy of the copolymers is decreased, which gave the narrow band gap as compared to the DMOP-PPV. The band gap of Oxa-PPV, DMOP-PPV, and Oxa-PPV-*co*-DMOP−PPV is about 2.41−2.34 eV. Figure 2 shows emission spectra of the Oxa-PPV, DMOP-PPV, and Oxa-PPV-*co*-DMOP-PPV thin films. When the polymer films were excited at the maximum absorption wavelength of each polymer, two emission peaks of DMOP-PPV are observed at 520 and 539 nm. However, as the Oxa-PPV content was increased in the copolymer systems, the emission peak is red-shifted from 520 to 573 nm. The photoluminescence excitation (PLE) spectra of Oxa-PPV, DMOP-PPV, and Oxa-PPV-*co*-DMOP-PPV were monitored at the λ_{max} of the emission spectrum of each polymer. The PLE spectra of Oxa-PPV, DMOP-PPV, and Oxa-PPV-*co*-DMOP-PPV are similar to the absorption spectrum. These phenomena indicated that the efficient energy transfer occurs from the 1,3,4-oxadiazole units to the PPV main chain.

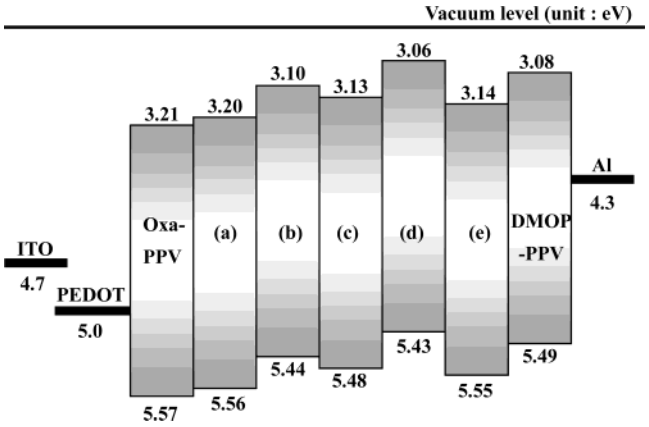

Figure 3. Hypothesized energy diagram of ITO/PEDOT/polymer/Al devices, Oxa-PPV, (a) Oxa-PPV-*co*-DMOP-PPV (84:16), (b) Oxa-PPV-*co*-DMOP-PPV (64:36), (c) Oxa-PPV-*co*-DMOP-PPV (51:49), (d) Oxa-PPV-*co*-DMOP-PPV (28:72), (e) Oxa-PPV-*co*-DMOP-PPV (7:93), and DMOP-PPV.

Cyclic voltammogram (CV) is a useful method for measuring electrochemical behaviors and evaluation of the relative HOMO, LUMO energy levels and the band gap of a polymer. During the anodic scan, the oxidation onset potentials of Oxa-PPV, DMOP-PPV, and Oxa-PPV-*co*-DMOP−PPV are in the range of 0.80−0.92 and exhibited irreversible p-doping processes. From the onset potential for the oxidation, the HOMO energy level of the polymers was estimated regarding the energy level of the FOC reference.[30] Figure 3 shows the hypothesized energy diagrams of the ITO/PEDOT/polymer/Al device fabricated in this work. HOMO energy levels of the present EL polymers are similar, and the values are about 5.43−5.57 eV. The LUMO energy level was calculated from the values of the band gap and HOMO energy level. The LUMO energy level of DMOP-PPV is 3.08 eV. However, as the 1,3,4-oxadiazole units in the copolymers were increased, the LUMO energy level was not increased. The LUMO energy level of 3.21 eV in Oxa-PPV is higher than that of CN-PPV (3.02 eV) and alkyl- or alkoxy-substituted PPV derivatives.[31] This means that the electrons are better injected into Oxa-PPV from the cathode metal than into CN-PPV and Oxa-PPV has an expected higher luminance efficiency than PPV derivatives when it is used as an emitting layer in PLEDs. The electrooptical data of the Oxa-PPV, DMOP-PPV, and Oxa-PPV-*co*-DMOP-PPV are summarized in Table 2.

Electroluminescence Properties and Current Density−Voltage−Luminescence (*J*−*V*−*L*) Characteristics. To decrease the operating voltage and smooth the surface roughness

(30) Leeuw, D. M.; Simenon, M. M. J.; Brown, A. R.; Einerhand, R. E. F. *Synth. Met.* **1997**, *87*, 53−59.
(31) Cervini, R.; Li, X. C.; Spencer, G. W. C.; Holmes, A. B.; Moratti, S. C.; Friend, R. H. *Synth. Met.* **1997**, *84*, 359−360.

Table 2. Absorption, PL, and EL Data of Oxa-PPV, DMOP-PPV, and Oxa-PPV-*co*-DMOP-PPV

polymer	abs_{max} (nm)	PL_{max} (nm)	EL_{max} (nm)	E_g (eV)[a]	HOMO (eV)[b]	LUMO (eV)
Oxa-PPV	441, 303	542,[c] 573	591	2.36	5.57	3.21
Oxa-PPV-*co*-DMOP-PPV (84:16)	443	542,[c] 573	570	2.36	5.56	3.20
Oxa-PPV-*co*-DMOP-PPV (64:36)	451	535, 571	534, 560	2.34	5.44	3.10
Oxa-PPV-*co*-DMOP-PPV (51:49)	457	533, 568	534, 560	2.35	5.48	3.13
Oxa-PPV-*co*-DMOP-PPV (28:72)	456	537	528,[c] 561	2.37	5.43	3.06
Oxa-PPV-*co*-DMOP-PPV (7:93)	449	520,[c] 558	528,[c] 561	2.41	5.55	3.14
DMOP-PPV	454	520, 539	513, 539	2.41	5.49	3.08

[a] Determined from the edge of the absorption spectrum. [b] Determined from the onset of the anodic scan of cyclic voltammetry. [c] Shoulder.

of the indium tin oxide (ITO) electrode, the hole injection-transport layer, poly(3,4-ethylenedioxythiophene) doped with poly(styrenesulfonate) (PEDOT/PSS), was spin-coated onto the surface-treated ITO substrate and dried on a hot plate for 30 min at 110 °C. The emissive layer was successively built up by spin casting on the top of the PEDOT layer. An aluminum electrode was deposited by evaporation at a pressure of 10^{-6} Torr. The current density−voltage (a) and luminescence−voltage (b) characteristics of ITO/PEDOT/polymer/Al devices are shown in Figure 4. The turn-on voltages of ITO/PEDOT (25 nm)/DMOP-PPV (80 nm)/Al and ITO/PEDOT (25 nm)/Oxa-PPV (80 nm)/Al devices are about 2.5 and 5 V, respectively. The copolymers showed a turn-on voltage similar to that of Oxa-PPV. The luminescence intensities of Oxa-PPV, DMOP-PPV, and Oxa-PPV-*co*-DMOP-PPV are exponentially increased with an increase in voltage. The maximum luminescence (L_{max}) of DMOP-PPV is 1840 cd/m^2 at 10 V. However, the maximum luminescence of copolymers dramatically increased with an increase in the feed ratios of Oxa-PPV, and the maximum luminescence of Oxa-PPV-*co*-DMOP-PPV (84:16), Oxa-PPV-*co*-DMOP-PPV (64:36), and Oxa-PPV-*co*-DMOP-PPV (51:49) is about 6500 cd/m^2. Oxa-PPV with an Al electrode shows a maximum luminescence of 19395 cd/m^2 at a voltage of 14 V. The device performance characteristics of double-layer devices are tabulated in Table 3.

Figure 5 shows the EL spectra of ITO/PEDOT/polymer/Al devices. The EL spectra are similar to their PL spectra. This result indicates that the EL and PL phenomena originated from the same excited state. The maximum EL peak of Oxa-PPV is red-shifted by 18 nm as compared to the PL spectrum. This change in EL spectrum is due to the injected current density, which results in an extended effective conjugation length. To investigate the color purity, chromaticity coordinates using the Commision International l'Eclairage (CIE) (1931) color matching function were converted from the EL spectrum, and the results are listed in Table 3. The emission colors of Oxa-PPV and DMOP-PPV at the CIE coordinates of $x = 0.50$, $y = 0.47$ and $x = 0.36$, $y = 0.55$ are yellowish-orange and green. By adjusting the feed ratios of Oxa-PPV in the copolymers, we could tune the emission colors from green to yellowish-orange.

Figure 6 shows the luminance efficiency of Oxa-PPV, DMOP-PPV, and Oxa-PPV-*co*-DMOP-PPV as a function of current density. As the 1,3,4-oxadiazole content in the copolymers was increased, the luminance efficiency of Oxa-PPV-*co*-

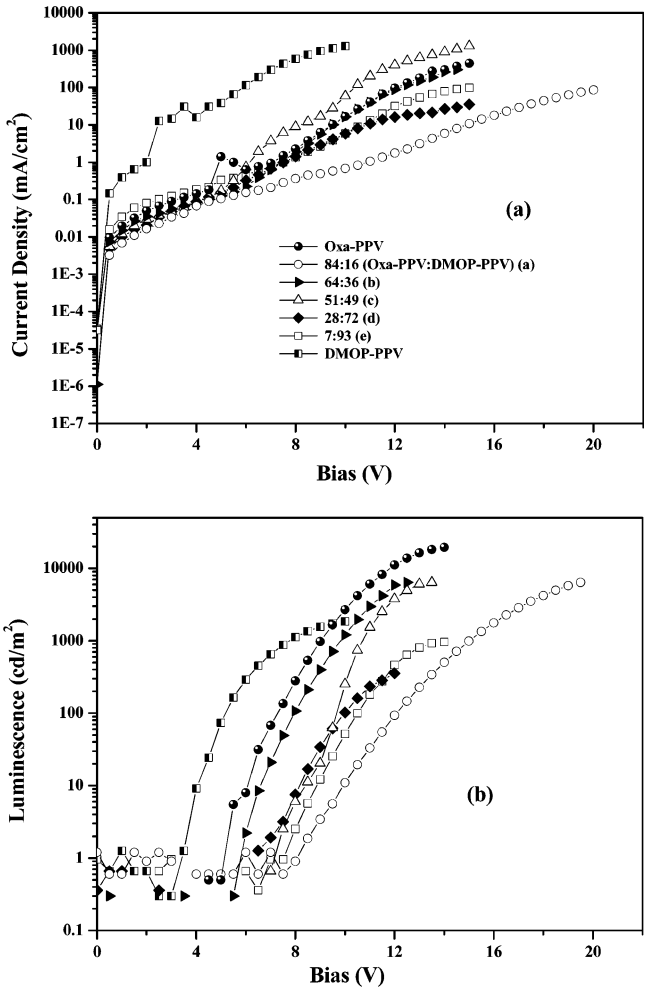

Figure 4. Current density−voltage−luminescence ($J-V-L$) characteristics of ITO/PEDOT/polymer/Al devices.

DMOP-PPV (84:16) was 41 times higher than that of DMOP-PPV and reached about 10 cd/A at 1760 cd/m^2 and 17 mA/cm^2. The luminance efficiency of Oxa-PPV containing 1,3,4-oxadiazole side groups was 21.1 cd/A at 5930 cd/m^2 and 29 mA/cm^2 based on double-layer PLEDs using an Al electrode and was 88 times higher than that of DMOP-PPV. The highest luminance efficiency of copolymers with a relatively low current density is due to the high LUMO energy level as compared to that of conventional PPV derivatives. The barrier heights of Oxa-PPV and Oxa-PPV-*co*-DMOP-PPV (84:16) were found to be 1.09 and 1.1 eV at the interface of the Al/LUMO state for electron injection. Thus, easily injected electrons were recombined with the holes in the emitting layer to give high luminance efficiency. The Oxa-PPV system also seems to form another charge transport channel (mainly for electrons) via wave-function overlapping of π-electrons along the 1,3,4-oxadiazole pendants itself as well as original transport (mainly for holes) along the PPV backbone. In fact, the suggestion of new π-electron channels is strongly supported by the observation of a broad spectral feature around 300 nm in the absorption spectrum of Oxa-PPV, which reflects π-electron wave-function overlapping along the 1,3,4-oxadiazole units. Therefore, we consider that the excellent performance of Oxa-PPV is also attributed to enhanced electron transport along new transport channels as well as easier electron injection in this system. Accordingly, introduction of 1,3,4-oxadiazole units into the PPV

Table 3. Device Performance Characteristics of Oxa-PPV, DMOP-PPV, and Oxa-PPV-*co*-DMOP-PPV

polymer	turn-on (V)	LE_{max},[a] cd/A	L_{max},[b] cd/m^2 (V)	CIE (x, y)[c]
Oxa-PPV	5	21.1 (29 mA, 5930 cd/m^2)	19395 (14 V)	(0.50, 0.47)
Oxa-PPV-*co*-DMOP-PPV (84:16)	7	10.0 (17 mA, 1760 cd/m^2)	6447 (18 V)	(0.47, 0.50)
Oxa-PPV-*co*-DMOP-PPV (64:36)	5.5	7.6 (26 mA, 1960 cd/m^2)	6430 (12 V)	(0.44, 0.52)
Oxa-PPV-*co*-DMOP-PPV (51:49)	5.5	0.62 (119 mA, 740 cd/m^2)	6370 (13 V)	(0.43, 0.53)
Oxa-PPV-*co*-DMOP-PPV (28:72)	6	2.2 (10.9 mA, 233 cd/m^2)	377 (12 V)	(0.44, 0.52)
Oxa-PPV-*co*-DMOP-PPV (7:93)	6.5	1.54 (42.5 mA, 640 cd/m^2)	980 (14 V)	(0.45, 0.51)
DMOP-PPV	2.5	0.24 (65.6 mA, 164 cd/m^2)	1840 (10 V)	(0.36, 0.55)

[a] Maximum luminescence. [b] Maximum luminance efficiency. [c] Calculated from the EL spectrum.

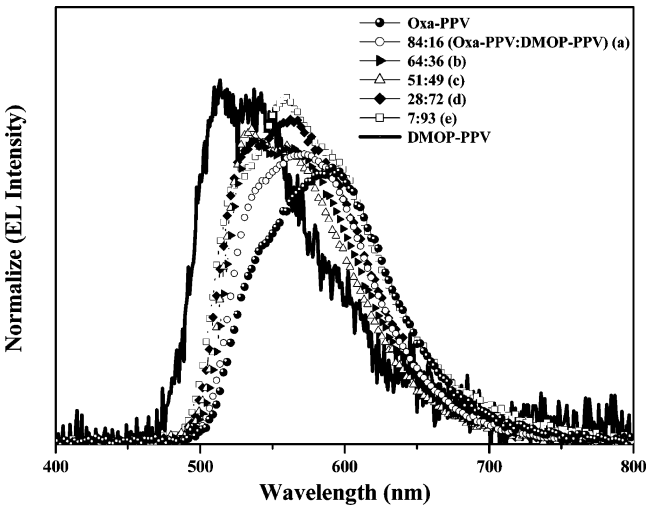

Figure 5. Electroluminescence spectra of ITO/PEDOT/polymer/Al devices.

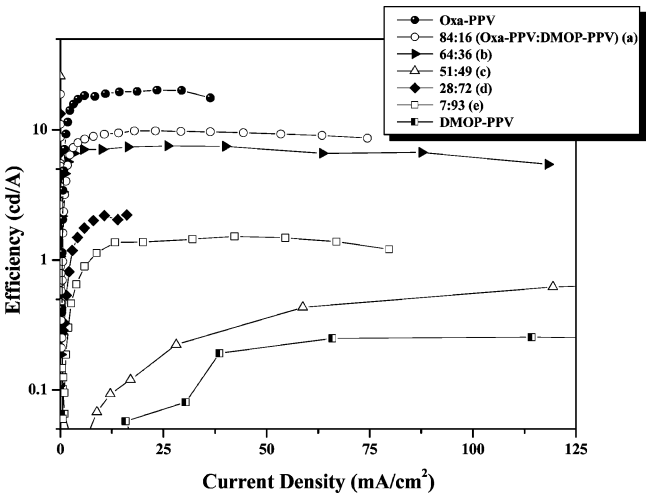

Figure 6. Luminance efficiency as a function of current characteristics of ITO/PEDOT/polymer/Al devices.

backbone via oxygen linkage and asymmetric molecular design of Oxa-PPV and Oxa-PPV-*co*-DMOP-PPV are responsible for the outstanding device performance.

Conclusions

This study focused on the design and synthesis of asymmetric PPV-based homopolymers as well as copolymers containing new chemically modified 1,3,4-oxadiazole derivatives through Gilch polymerization of PLEDs. The resulting EL polymers with high molecular weights exhibited good solubility in conventional organic solvents, which make high-quality optical thin films, and high glass transition temperatures. Electrooptical properties and device performance can be easily controlled by properly adjusting the feed ratios of the Oxa-PPV content in copolymers. From the absorption and emission spectra, these polymers emit green to yellowish-orange with a band gap of 2.34−2.41 eV. Introduction of an electron-deficient 1,3,4-oxadiazole unit into the PPV backbone as the side chain enhances the electron affinity and increases the LUMO energy level, which facilitate the improvement of device performance. Turn-on voltages of the present EL polymers with ITO/PEDOT/polymer/Al devices were in the range of 2.5−7 V. As the Oxa-PPV content was increased in copolymers, the device performance was significantly increased as compared to that of DMOP-PPV. The maximum brightness and luminance efficiency of the present EL polymers were 19395 cd/m^2 at 14 V and 21.1 cd/A at 5930 cd/m^2. The improved device performance of Oxa-PPV over those of DMOP-PPV and Oxa-PPV-*co*-DMOP-PPV is due to the better electron injection and efficient energy transfer from the modified 1,3,4-oxadiazole side group to the PPV main chain. This is the first report concerning the high brightness and high luminance efficiency at high operating luminescence even though the Al electrode and these polymers are promising materials for PLEDs.

Acknowledgment. This work was supported by a Korea Research Foundation Grant (KRF-2002-015-CS0028).

Supporting Information Available: Experimental spectra (PDF). This material is available free of charge via the Internet at http://pubs.acs.org.

JA036955+